



HAL
open science

Microscale thermal characterization at temperatures up to 1000 ° C by photoreflectance microscopy. Application to the characterization of carbon fibres

Denis Rochais, H el ene Le Hou edec, Franck Enguehard, Julien Jumel, Fran ois Lepoutre

► To cite this version:

Denis Rochais, H el ene Le Hou edec, Franck Enguehard, Julien Jumel, Fran ois Lepoutre. Microscale thermal characterization at temperatures up to 1000 ° C by photoreflectance microscopy. Application to the characterization of carbon fibres. *Journal of Physics D: Applied Physics*, 2005, 38 (10), pp.1498-1503. 10.1088/0022-3727/38/10/002 . hal-01287446

HAL Id: hal-01287446

<https://hal.science/hal-01287446>

Submitted on 22 Dec 2022

HAL is a multi-disciplinary open access archive for the deposit and dissemination of scientific research documents, whether they are published or not. The documents may come from teaching and research institutions in France or abroad, or from public or private research centers.

L'archive ouverte pluridisciplinaire **HAL**, est destin ee au d ep ot et  a la diffusion de documents scientifiques de niveau recherche, publi es ou non,  emanant des  tablissements d'enseignement et de recherche fran ais ou  trangers, des laboratoires publics ou priv es.

Microscale thermal characterization at temperatures up to 1000°C by photoreflectance microscopy. Application to the characterization of carbon fibres

D Rochais¹, H Le Houédec¹, F Enguehard¹, J Jumel¹ and F Lepoutre²

¹ CEA Le Ripault, BP 16—37260 Monts, France

² ONERA, DMSE/MECS, BP 72—29 av division Leclerc, 92322 Châtillon, Cedex, France

Micrometric scale thermal diffusivity measurement by photoreflectance microscopy is now a well-known technique. Until now the experiments were performed essentially at room temperature. In this paper we explore temperature resolved tests. We describe the modifications introduced in the experimental set-up and the procedure followed to determine the temperature dependent diffusivity. Different analysis methods are described and first tests performed on known materials and a C/C composite is presented.

1. Introduction

C/C composites are made of several micro-components [1] whose properties are often not known precisely as a function of temperature. Such a lack of knowledge makes it difficult to use multi-scale numerical simulations that require reliable microscopic data [2] to predict the influence of individual micro-parameters on the macroscopic thermal properties. Because of the size of the constituents, conventional methods are not suitable; only photoreflectance microscopy [3] has the required spatial resolution to determine precisely the thermal properties of a carbon fibre with a material volume as small as a few cubic micrometres in diameter. This purely optical method is based on the measurement of the thermally induced variation of the sample reflection coefficient [4, 5]. From the analysis of the experimental data, the local thermal properties are deduced [6].

Until now, C/C composites were characterized with this technique only at room temperature [7] whereas thermal diffusivity measurements at various temperatures have already been performed by infrared microscopy with a 30 μm spatial resolution [8]. Our purpose is to measure the thermal diffusivities of the constituents of C/C composites heated at temperatures up to 1000°C. After presenting the modifications

we have introduced in our photothermal microscope to perform these experiments, we describe the experimental procedure that we follow to determine the evolution of the thermal diffusivity of a material with temperature at a microscopic scale. To show the possibilities inherent in this method, we present first the results for two well-known materials (molybdenum and chromium) and second the results for a PAN-based carbon fibre at 1000°C.

2. Microscopic thermal characterization by photoreflectance microscopy

Photothermal microscopy is based on the measurement and analysis of the periodic temperature increase induced by the absorption of an intensity-modulated laser beam (pump beam). By detecting the variations of the thermally induced reflection coefficient with the help of a secondary continuous laser beam (probe beam), the local temperature increase at the sample surface can be measured. Thermal parameters are then identified by fitting the periodic signal to a suited model. Unlike other photothermal methods, this contactless technique has a micrometric spatial resolution.

2.1. Thermal wave propagation

When an isotropic, homogeneous medium is heated by a periodic point-like heat source of power Q , the periodic temperature increase, also called ‘thermal wave’, at a distance r from the pump location is described by the following equation:

$$\delta T(r, t) = \frac{Q}{4\pi kr} \exp\left(-\frac{r}{\mu}\right) \cos\left(\omega t - \frac{r}{\mu}\right), \quad (1)$$

where

$$\mu = \sqrt{\frac{\alpha}{\pi f}} \quad (2)$$

is called the thermal diffusion length, f being the modulation frequency of the harmonic heat source, $\alpha = k/\rho C$ the thermal diffusivity of the material, k its thermal conductivity, and ρC its volume specific heat. Equation (1) holds when the size of the pump beam is small compared to the thermal diffusion length. We note that the thermal waves are damped: the higher the modulation frequency, the sharper the periodic temperature decrease. At a few hundreds of kilohertz and for usual thermal diffusivity values (smaller than $10^{-4} \text{ m}^2 \text{ s}^{-1}$), the thermal wave is confined in a volume of a few cubic micrometres. It can be seen that the phase shift $\varphi = -r/\mu$ between the periodic temperature rise at the surface of the medium and the modulation of the heat source decreases linearly as the distance from the heat source r increases. The slope of the phase curve along r is constant and equal to $-1/\mu$. Thus, the recording of this curve measure enables us to evaluate easily the thermal diffusivity by a linear fit using equation (2). Nevertheless, the focused pump beam energy distribution, which limits the spatial resolution of the measurements [6], must be taken into account to determine the thermal diffusivity precisely.

2.2. Photoreflectance measurement principle and experimental set-up

To perform a photothermal experiment at such a local scale, the only available technique is photoreflectance microscopy [3]. It consists in measuring with a photodiode the light flux of a continuous laser beam (intensity I_0), called the probe beam, after it has been reflected on the sample surface in the periodically heated zone. If the temperature variation is small, the reflection coefficient of the surface can be assumed to vary linearly with temperature according to relation (3) [9]:

$$\delta R(r, t) = R_0 \left[1 + \frac{1}{R_0} \frac{\partial R}{\partial T} \delta T(r, t) \right]. \quad (3)$$

After reflection, the ac component of the probe beam intensity $\delta I(r, t)$ is directly proportional to the temperature increase:

$$\delta I(r, t) = R_0 I_0 \left[\frac{1}{R_0} \frac{\partial R}{\partial T} \delta T(r, t) \right]. \quad (4)$$

These intensity variations can be detected with a photodiode whose signal is filtered by a lock-in amplifier. The amplitude of the signal depends on both thermal and optical parameters; on the other hand, the phase term is independent of optical artefacts and depends only on the thermal diffusivity of the material.

The experimental set-up, described in figure 1, consists of three main parts: an optical set-up for focusing and positioning the pump and probe beams, a device for measuring the reflected probe beam intensity, and several electronic devices for detecting the signal and driving the experiment.

The pump beam is a continuous Ar^+ laser whose maximum power is 2 W. Its intensity is modulated by a

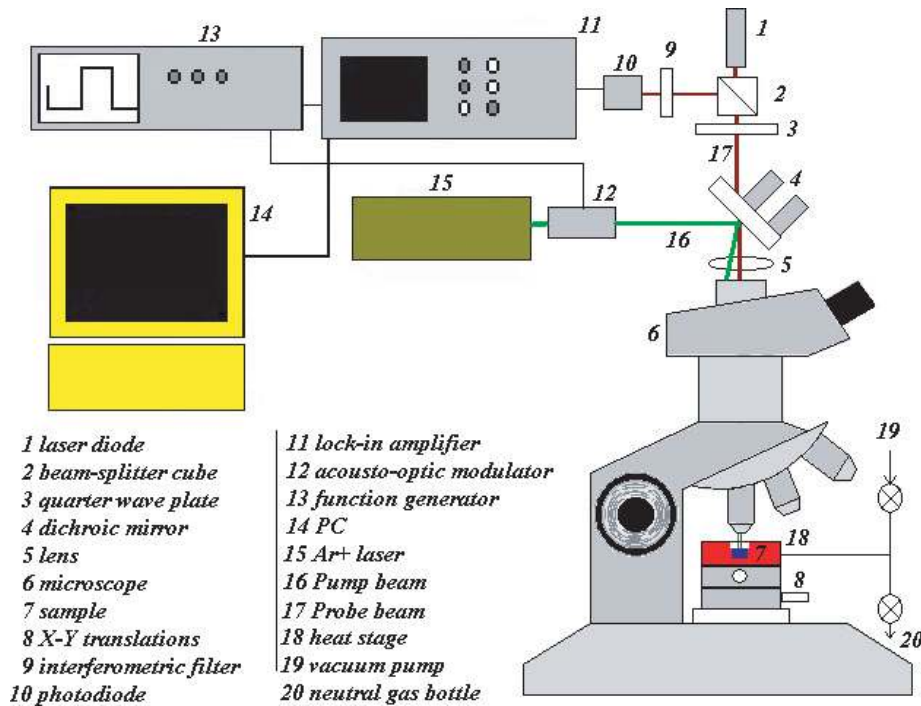


Figure 1. Thermal microscope set-up.

frequency generator-driven acousto-optic modulator operated at frequencies up to 2 MHz. The pump beam is then directed by a dichroic mirror and finally focused onto the sample surface in the heating stage with a microscope.

The probe beam is a laser diode (wavelength 780 nm, power 20 mW) that travels through a quarter-wave plate and the dichroic mirror, and is then focused onto the sample surface with the same microscope. After reflection, it travels through the quarter-wave plate again and is then sent to the photodiode by a beam splitter cube. An optical filter prevents any pump beam photon from reaching the detector.

A lock-in amplifier extracts the amplitude and phase of the periodic signal collected by the photodiode. A PC controls the dichroic mirror orientation and, consequently, the distance r between the probe and pump beam locations.

The heating stage window, made of fused silica, transmits 93% of the intensities of the two beams. An objective ($\times 40$) with a large work distance specially designed to correct the spherical aberrations due to the heating stage window is used. The highest temperature that the heating stage can reach is 1500°C under a vacuum level better than 10^{-3} mbar.

A mirror polishing of the sample is necessary to ensure good reflection. The sample has a diameter less than 7 mm and a thickness around 1 mm. Its thickness must be as small as possible to avoid any temperature gradient in this direction caused by the heating and, thus, have a homogeneous sample temperature.

3. First high temperature tests

3.1. Isotropic material characterization

Tests were first performed on homogeneous and isotropic materials, which are easier to characterize. When heating the sample up to a few 100°C , new difficulties appear, such as a change in the surface aspect, oxidation, thermal expansion of the sample and a related defocusing of the laser beams. To avoid or at least reduce the oxidation that may appear during the measurements, we apply a primary vacuum sequence and then set a neutral gas circulation.

The procedure that we apply for temperature-resolved thermal characterizations can be described in several steps. First, we perform a two-dimensional scanning of the sample surface at room temperature. Figure 2 shows a typical result obtained on a molybdenum sample. We note that, in the vicinity of the pump beam, the isophase lines are a little elliptic: this is due to the probe beam, which is quite elliptic and induces an apparently anisotropic behaviour of the sample when the two beams are close to each other. But far enough from the pump beam, isophase lines become circular and one may exclude any thermal anisotropy in this case.

This experiment typically takes 8 h. Nevertheless, this tedious two-dimensional scanning operation is necessary for three reasons: first, it allows us to rapidly visualize the degree of thermal anisotropy of the sample, second, it permits us to identify the two thermal diffusion principal axes in the case of an anisotropic material, and third, it allows us to check that these principal axes are in the sample surface plane.

For isotropic materials, characterizations at higher temperatures are performed via one-dimensional scannings

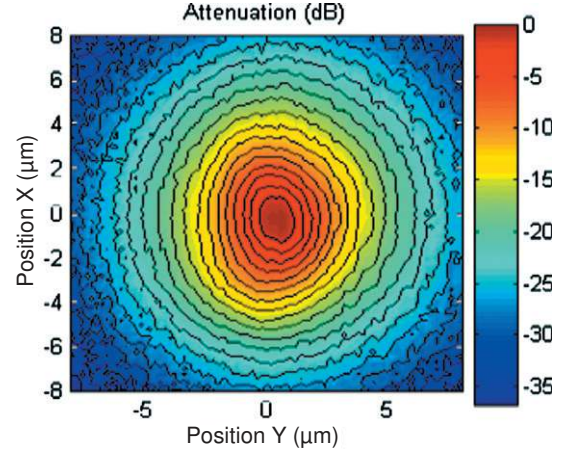


Figure 2. Two-dimensional amplitude scan at 300 kHz and 20°C collected on a molybdenum sample.

of the sample. The thermal diffusivity can be roughly estimated from the two slopes of the one-dimensional phase profile (section 2.1). Then, a complete model integrating the finite sizes of both the pump and the probe beams allows the determination of the thermal diffusivity. In the following two plots obtained for chromium (figure 3) at 750°C and molybdenum (figure 4) at 300°C (both materials being thermally isotropic), the crosses are the experimental data and the continuous lines are the calculated fits.

The thermal diffusivity of chromium at 750°C determined from figure 3 is $1.5 \times 10^{-5} \text{ m}^2 \text{ s}^{-1}$, i.e. exactly the value recommended in [10].

On the other hand, for molybdenum at 300°C , we find a diffusivity of $4.0 \times 10^{-5} \text{ m}^2 \text{ s}^{-1}$ from figure 4, whereas [10] recommends a value of $4.5 \times 10^{-5} \text{ m}^2 \text{ s}^{-1}$. The accuracy of our evaluation can be improved by a simultaneous adjustment of several profiles recorded at different modulation frequencies. This constitutes the third step, illustrated in figure 5 for the molybdenum sample at 300°C .

The diffusivity evaluated at figure 5 from the multi-frequency adjustment is found to be $4.3 \times 10^{-5} \text{ m}^2 \text{ s}^{-1}$. So the multi-frequency adjustment produces a result that is nearer to the one from the literature.

Figure 6 shows that we obtain, like in [10], a molybdenum diffusivity decreasing with temperature. We can note that our thermal diffusivity measurements determined by least squares adjustment are lower than the accepted values above 800°C . We think this discrepancy is due to the beginning of a surface oxidation observed above this temperature. Indeed, when we did these experiments, there was a leak in the neutral gas circulation circuit. Nevertheless, these first tests have demonstrated the ability of the photoreflectance technique to perform temperature dependent diffusivity measurements.

3.2. Anisotropic material characterization

A thermally anisotropic material is characterized by its thermal conductivity tensor \underline{K} , which is diagonal in the coordinate system defined by the three principal directions of anisotropy. If two of these directions, x and y , are parallel to the surface of the sample, and the z direction is normal to the surface of the sample, the temperature field induced by a point-like periodic heat source of power Q (anisotropic Green solution)

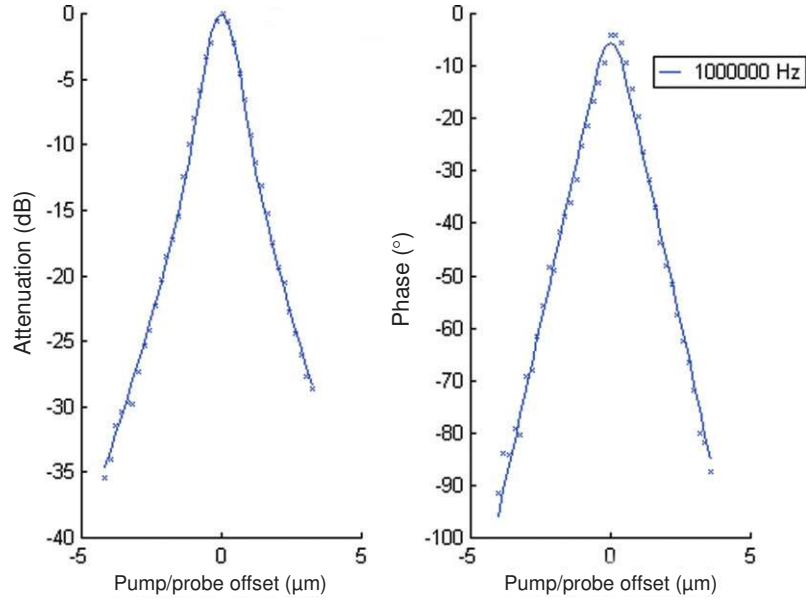


Figure 3. One-dimensional scan of chromium at 750°C and its related least square adjustment. The frequency is fixed and the radii identified are $r_{\text{pump}} = 0.85 \mu\text{m}$ and $r_{\text{probe}} = 1.23 \mu\text{m}$.

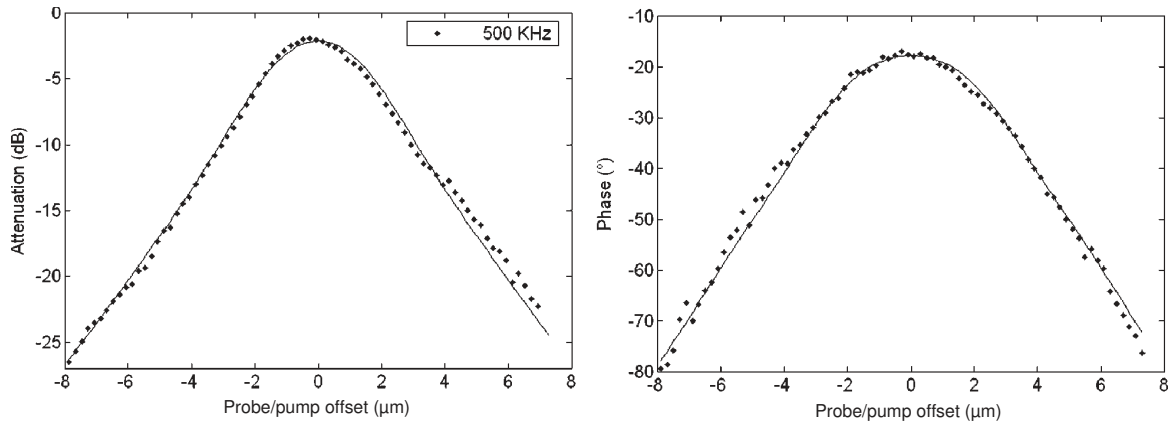


Figure 4. One-dimensional scan of molybdenum at 300°C and its related least square adjustment. The frequency is fixed and the radii identified are $r_{\text{pump}} = 1.12 \mu\text{m}$ and $r_{\text{probe}} = 1.66 \mu\text{m}$.

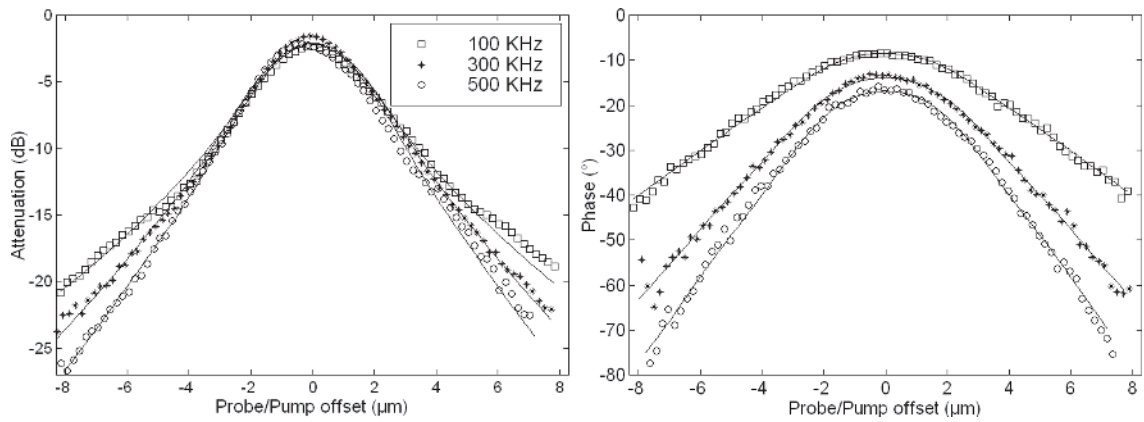


Figure 5. Thermal diffusivity determination of molybdenum at 300°C by simultaneous least square adjustment of several one-dimensional phase profiles collected at different frequencies. The radii identified are $r_{\text{pump}} = 1.11 \mu\text{m}$ and $r_{\text{probe}} = 1.61 \mu\text{m}$.

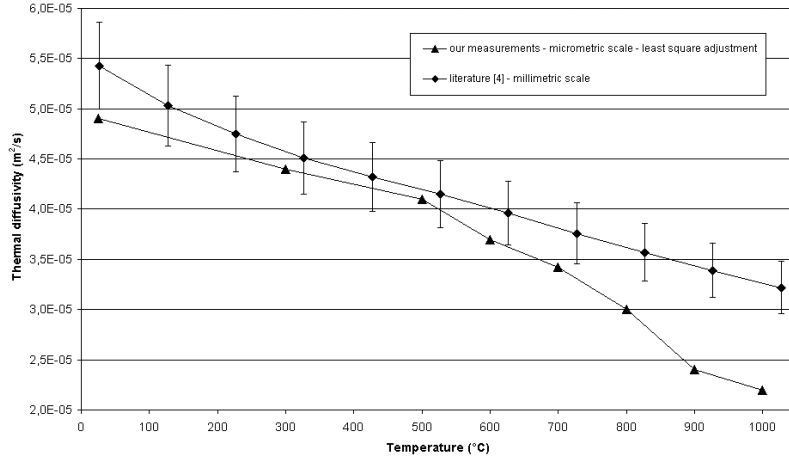


Figure 6. Thermal diffusivity of molybdenum versus temperature: comparison of our measurements to literature data.

is described by the following equation [11, 12]:

$$\delta T(x, y, z) = \frac{Q}{4\pi\sqrt{k_x k_y k_z} R} \exp(-(1+j)\sqrt{\pi f \rho C} R), \quad (5)$$

where

$$R(x, y, z) = \sqrt{\frac{1}{k_x} x^2 + \frac{1}{k_y} y^2 + \frac{1}{k_z} z^2}. \quad (6)$$

In these expressions, k_x , k_y and k_z are the thermal conductivities along the x , y and z directions. Isotherms are in this case elliptic, their ellipticity being equal to the square root of the thermal anisotropy k_x/k_y . The slopes of the phase curves of the periodic temperature increase along the principal directions of thermal anisotropy still enable, using relation (2), the determination of the corresponding principal thermal diffusivity values.

As in the case of isotropic materials, the actual energy distributions of the pump and probe beams can be taken into account to calculate the exact periodic temperature increase at the surface of a thermally anisotropic sample [11]. But practically, because of the number of parameters we need to adjust, we use the basic description of the periodic temperature elevation (equations (5) and (6)) to analyse the photoreflectance measurements that we perform on anisotropic materials [7].

3.2.1. Thermal parameters extraction scheme

3.2.1.1. Thermal diffusivity extraction from phase measurement. As in the isotropic case, we first focus on the phase measurement. According to relations (5) and (6), this measurement should allow us to extract two of the principal thermal diffusivities, provided that the corresponding principal axes of anisotropy are parallel to the sample surface. Indeed, the phase of the periodic temperature increase at the surface of the sample is given by

$$\varphi(x, y) = -\sqrt{\frac{x^2}{\mu_x^2} + \frac{y^2}{\mu_y^2}}. \quad (7)$$

The slope of the phase curve in a radial direction from the heating point is equal to

$$\frac{d\varphi}{dr}(\theta) = -\sqrt{\frac{\cos(\theta)^2}{\mu_x^2} + \frac{\sin(\theta)^2}{\mu_y^2}}, \quad (8)$$

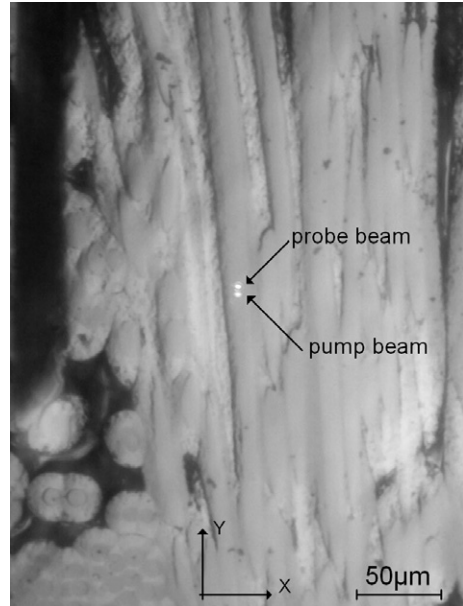


Figure 7. Photograph of the scanning zone of the composite obtained at 1000°C.

where θ is the polar angle between the x and radial directions.

From the slope of the phase along the two principal thermal directions of anisotropy one can deduce the corresponding principal thermal diffusivities. To make full use of the numerous experimental data points, we reconstruct the radial phase profiles, then calculate the phase slopes for several orientations θ and fit these values with relation (8).

3.2.1.2. Thermal anisotropy extraction from amplitude measurement. Like the isophase lines, the isoamplitude lines are also elliptic. Their ellipticity degree is also equal to the square root of the thermal anisotropy. We use this property to extract the thermal anisotropy applying a best fit procedure to the experimental elliptic isoamplitude lines. Indeed, Jumel [13] has demonstrated that an evaluation of the thermal anisotropy based on the isoamplitude lines provides a lower uncertainty (better than 10%) than an evaluation based on isophase lines, which are more sensitive to convolution effects.

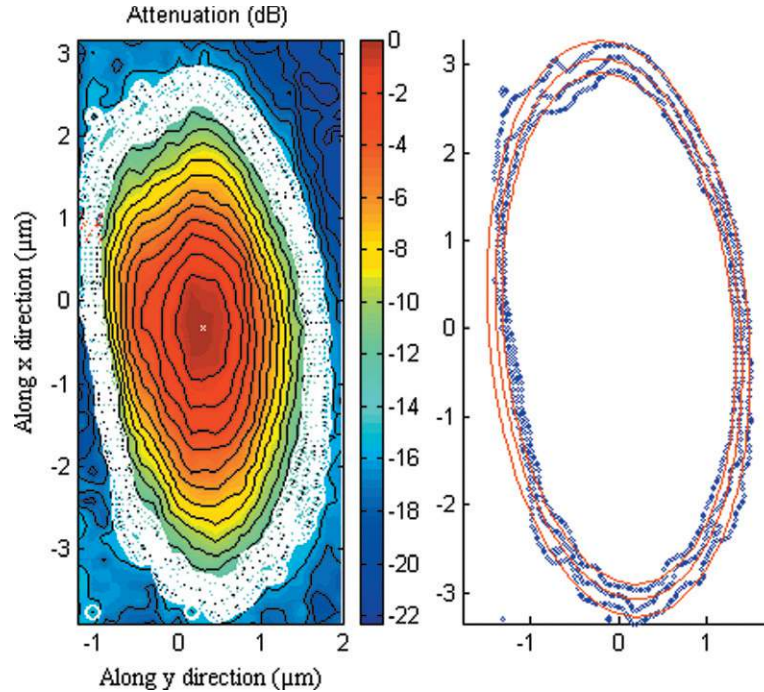


Figure 8. Isoamplitude line fit result after a two-dimensional scanning of a carbon fibre at 1000°C. The thermal anisotropy determined is 5.

3.3. Carbon fibre characterization at 1000°C

Using our photothermal microscope and the previously described thermal parameter extraction scheme, we measured the thermal diffusivity tensor of a PAN-based carbon fibre within a three-dimensional C/C composite heated at 1000°C. Figure 7 shows a photograph of the scanning zone obtained at 1000°C. The fibres, whose diameter is generally smaller than 8 µm, are supposed to be transversally isotropic. We have chosen to characterize one of these fibres, cut along its longitudinal section (cf figure 7). As carbon is very sensitive to oxidation when the temperature increases, we have conducted our experiments at a vacuum level of 10^{-3} mbar. Figure 8 shows an isoamplitude line fit result after a two-dimensional scanning of the carbon fibre surface at 1000°C. The anisotropy level determined in this way is 5. Moreover, the maximum thermal diffusivity (longitudinal) mean value extracted from the phase measurements is equal to $1.3 \times 10^{-5} \text{ m}^2 \text{ s}^{-1}$, while the smallest one (transversal), deduced from the thermal anisotropy derived from the amplitude measurements, is $2.6 \times 10^{-6} \text{ m}^2 \text{ s}^{-1}$. The longitudinal thermal diffusivity determined *in situ* can be compared to those found at 1000°C by Pradère [14] for a similar PAN-based carbon fibre alone (i.e. *ex situ*): $1.0 \times 10^{-5} \text{ m}^2 \text{ s}^{-1}$ to $3.0 \times 10^{-5} \text{ m}^2 \text{ s}^{-1}$ depending on the heat treatment applied to the carbon fibre before characterization.

4. Conclusion

Photoreflectance microscopy allows the determination of micrometric scale thermal diffusivity as a function of temperature. The choice of the analysis method (two-dimensional

scanning, least squares adjustment of one or several one-dimensional phase profiles) depends on the material studied, the accuracy desired for the characterization, the temperature level and the time available. The next step will be the study of the composite constituents (matrix and fibres) at temperatures up to 1500°C, which is the maximum temperature allowed by our heating stage.

References

- [1] Legendre A 1992 *Le matériau carbone* (Paris: Eyrolles)
- [2] Klett J W, Ervin V J and Edie D D 1999 *Comput. Sci. Technol.* **59** 593–607
- [3] Potier L 1994 *Appl. Phys. Lett.* **64** 1618–19
- [4] Opsal J and Rosencweig A 1982 *J. Appl. Phys.* **53** 4240
- [5] Rosencweig A, Opsal J, Smith W L and Willenborg D L 1985 *Appl. Phys. Lett.* **46** 1013–15
- [6] Lepoutre F, Balageas D, Forge Ph, Hirschi S, Joulaud J L, Rochais D and Chen F C 1995 *J. Appl. Phys.* **78** 2208–23
- [7] Jumel J, Lepoutre F, Enguehard F, Rochais D and Cataldi M 2001 *High Temperature Ceramic Matrix Composites Conf. (Munich, Germany) AIP Conf. Proc.* **615** 1439
- [8] Bisson J F and Fournier D 1998 *High Temp.— High Pressures* **30** 205–10
- [9] Velinov T 1995 *Meas. Sci. Technol.* **6** 28–32
- [10] Touloukian Y S, Powell R W, Ho C Y and Nicolaou M C 1973 *Thermophysical Properties of Matter* vol 10 (New York, Washington: IFI/Plenum)
- [11] Vaez Iravani M and Nikoonahad M 1987 *J. Appl. Phys.* **62** 4065–71
- [12] Chang Y P, Kang C S and Chen D J 1972 *Int. J. Heat Mass Transfer* **16** 1905–18
- [13] Jumel J 2003 *PhD Dissertation* Ecole Normale Supérieure de Cachan, France
- [14] Pradère C 2004 *PhD Dissertation* Ecole Nationale Supérieure d'Arts et Métiers, France